Biofabrication

PAPER

Autonomous spheroid formation by culture plate compartmentation

Marian Fürsatz[1,2], Peter Gerges[2,3], Susanne Wolbank[2,4] and Sylvia Nürnberger[1,2,4]

[1] Department of Orthopedics and Trauma-Surgery, Division of Trauma-Surgery, Medical University of Vienna, Vienna, Austria
[2] Ludwig Boltzmann Institute for Experimental and Clinical Traumatology, AUVA Research Centre, Vienna, Austria
[3] Institute of Applied Physics, Vienna University of Technology, Vienna Austria
[4] Austrian Cluster for Tissue Regeneration, Vienna, Austria

E-mail: sylvia.nuernberger@meduniwien.ac.at

RECEIVED
10 October 2020

REVISED
25 December 2020

ACCEPTED FOR PUBLICATION
29 January 2021

PUBLISHED
7 April 2021

Keywords: autonomous spheroid formation, chondrogenic differentiation, compartmentalisation, co-culture, micromass pellets, pellet culture, self-assembling

Supplementary material for this article is available online

Abstract

Scaffold-free 3D cell cultures (e.g. pellet cultures) are widely used in medical science, including cartilage regeneration. Their drawbacks are high time/reagent consumption and lack of early readout parameters. While optimisation was achieved by automation or simplified spheroid generation, most culture systems remain expensive or require tedious procedures. The aim of this study was to establish a system for resource efficient spheroid generation with additional early readout parameters. This was achieved by a new approach for spheroid generation via self-assembly from monolayer via compartmentation of cell culture surfaces utilising laser engraving (grid plates). The compartmentation triggered contraction and rolling up of the cell monolayer, finishing in condensation into a spheroid in human adipose-derived stem cell (ASC/TERT1) and human articular chondrocytes (hACs)-ASC/TERT1 co-cultures, when cultivated on grid plates under chondrogenic conditions. Plates with 1 and 3 mm grid size yielded stable diameters (about 140 μm and 300 μm, respectively). ASC/TERT1 spheroids fully formed within 3 weeks while co-cultures took 1–2 weeks, forming significantly faster with increasing hAC ratio ($p < 0.05$ and 0.01 for 1:1 and 1:4 ASC/TERT1:hAC ratio, respectively). Co-cultures showed slightly lower spheroid diameters, due to earlier spheroid formation and incomplete monolayer formation. However, this was associated with a more homogeneous matrix distribution in the co-culture. Both showed differentiation capacity comparable to standard pellet culture in (immune-)histochemistry and RT-qPCR. To assess usability for cartilage repair, spheroids were embedded into a hydrogel (fibrin), yielding cellular outgrowth and matrix deposition, which was especially pronounced in co-cultures. The herein presented novel cell culture system is not only a promising tool for autonomous spheroid generation with the potential of experimental and clinical application in tissue engineering, but also for the generation of 'building blocks' for subsequential biofabrication strategies such as bioprinting.

1. Introduction

Scaffold-free high cell density cultures have been extensively used in tissue engineering and many other fields of medical science. The most frequently used culture types are: (a) hanging drop culture, (b) pellet culture and (c) micromass culture. (a) Hanging drop culture is the typical system for a variety of different setups from cancer research to differentiation studies [1–3]. However, handling can be challenging since evaporation and limited possibility of media exchange often require transfer of the generated pellets to well plates for longer culture times. (b) Pellet cultures are the gold standard for chondrogenic differentiation [4, 5] but are also used for generation of other organoids in fields such as bone and cancer research [3, 6]. Historically, pellet cultures were established in rather big vessels (e.g. 15 ml centrifugation

© 2021 IOP Publishing Ltd

tubes or Eppendorf tubes), which led to high consumption of media, laborious maintenance during the condensation stage (e.g. media change of multiple vials), and the need for an additional transfer of pellets to well plates or vials for long-term maintenance of cultures. This has to some extent been alleviated by using 96-well plates made out of materials which are inherently less adhesive, or by blocking cell adherence using compounds such as agarose or poly(2-hydroxyethyl methacrylate) (poly-HEMA), which is often referred to as liquid overlay technique [7]. Nevertheless, time and media consumption still leave much room for optimisation. (c) Micromass culture differs from the other two methods, as it does not predominantly form pellets by gravity. Here, cells are seeded at high density in small drops on the bottom of wells forming nodules [8] or in some cases spheroids [5]. While previously used for developmental studies [9], it has more recently been used for drug testing and chondrogenic differentiation [5, 8]. In general, this method is used far less often than the others mentioned above, as it usually produces inhomogeneous shapes and sizes.

The disadvantages of all these methods are their time-intensive handling, high reagent consumption and lack of early readout parameters. An efficient way to alleviate these drawbacks is partial or total automation of spheroid generation, maintenance and analysis. Many automated systems use the hanging drop culture for spheroid generation. Tung *et al.* [10] presented a custom made hanging drop plate design, which allowed automated spheroid generation and maintenance of molarity for up to 2 weeks. This was achieved by holes in the plate enabling access to the drop from above, therefore allowing for easier media changing while also introducing additional reservoirs to minimise evaporation. Other systems, while employing slightly different plate designs and liquid handling systems, use similar approaches to achieve hanging drop automatisation [11–13]. However, none of the publications showed cultivation times longer than 2 weeks, and spheroid transfer to standard well plates was still required for further cultivation. Additionally the generated spheroid size is limited by the achievable drop size, which can only be increased by special plate designs until a certain point before masses become too large to maintain a hanging droplet.

For pellet culture, earlier approaches mainly attempted to simplify pellet generation (e.g. using pipetting automates to distribute cell solutions homogeneously into multi-well plates and let them aggregate by sedimentation or subsequent manual centrifugation) [14]. Newer systems strive for all-in-one solutions, often including automatised analysis (e.g. automated staining, fluorescence imaging and flow cytometry). With these systems, fully automated hanging drop and pellet cultures could be performed [15, 16] and additional incorporation of nanoparticles (e.g. magnetic) improved functionality and handling [17].

While all of these methods achieve automation and therefore vastly improve the amount of workhours and reagents used, the necessary equipment has high acquisition and maintenance costs, which makes them often unaffordable or uneconomic, especially for smaller labs. Micro-moulding [18–21] and surface patterning [22] have been explored as alternatives for generation of high quantities of micromass pellets with highly repeatable size and morphology. Some of these methods allow for the design of interestingly shaped cell constructs, such as honeycombs [18], which could provide new options for application in regenerative medicine. However, most of these methods depend on laborious production of culture vessels (e.g. multistep casting procedures) [21, 23] and are not easily integrated into standard culturing vessels.

Therefore, we developed an easily mass-producible culturing system for autonomous spheroid formation on compartmented surfaces, using standard cell culturing vessels (e.g. 60 mm Petri dishes). Compartmentation is achieved by computer-guided laser engraving, which allows for highly reproducible patterning and high-speed manufacturing. Chondrocytes and adipose-derived stromal cells were used either in mono- or co-culture to test the feasibility for chondrogenic spheroid generation. Since all spheroids are generated within one dish, the effects of pipetting errors and time for media changes are significantly reduced compared to standard pellet culture approaches in 96-well plate format. Further, due to the reduced media volume required in Petri dishes compared to well plates, reagent costs for spheroid generation and maintenance can be significantly reduced. The kinetics of spheroid formation provide further readouts, available before the endpoint of cultivation. This early readout option is a promising tool for pharmaceutical high-throughput screening or may be used for developmental research. Additionally, the system might also be used to generate spheroids for cell therapy and tissue engineering applications.

2. Material and methods

2.1. Cells and media

Human articular chondrocytes (hACs) were isolated from human femur heads obtained from joint replacements. The study was approved by the local ethics committee, and patient consent was given via a consent form. Human telomerase reverse transcriptase immortalised adipose-derived stem cells (ASC) (ASC/TERT1) were obtained from Evercyte GmbH (Austria, Vienna). Expansion and chondrogenic differentiation media were used as previously described [24]. Briefly, chondrocyte expansion media (CM) consisted of DMEM high glucose (Gibco,

41966-029), 10% FCS (PAN Biotech), 2 μg ml^{-1} amphotericin B (Gibco), 100 μg ml^{-1} gentamicin (Gibco), 50 μg ml^{-1} L-ascorbic acid 2-phosphate (Sigma-Aldrich), 10 mM HEPES, 5 μg ml^{-1} insulin (Sigma-Aldrich) and 2 mM L-glutamine (Gibco). EGM-2 was used for ASC/TERT1 expansion while retaining chondrogenic potential as previously described [24] (EBM-2 basal medium + EGM-2 BulletKit) and was purchased from Lonza. Chondrogenic differentiation medium with a low dose of growth factors was chosen. It contained DMEM high glucose (Sigma-Aldrich D6546), 5 mg ml^{-1} insulin and transferrin and 5 ng ml^{-1} selenous acid provided as ITS premix (Gibco), 0.17 mM L-ascorbic acid 2-phosphate, 1 mM sodium pyruvate (Gibco), 0.35 mM L-proline (Sigma-Aldrich), 1.25 mg ml^{-1} bovine serum albumin (Sigma-Aldrich), 100 U ml^{-1} penicillin/streptomycin (Gibco) and 2 mM L-glutamine (Gibco), and was freshly supplemented with 20 nM dexamethasone (Sigma-Aldrich), 1 ng ml^{-1} rhTGFβ-3 (R&D Systems, 243-B3/CF) and 1 ng ml^{-1} rhBMP-6 (R&D Systems, 507-BP) at use.

2.2. Isolation and cultivation of hAC

For the isolation of primary hAC, cartilage was taken from non-arthritic regions of femoral heads and cut into ~1–2 mm^3 pieces, followed by 30 min incubation in antibiotic solution (0.5 mg ml^{-1} gentamicin, 10 μg ml^{-1} amphotericin B). Cartilage was then digested for 30 min in 1 mg ml^{-1} hyaluronidase (Sigma), 1 h in 1 mg ml^{-1} pronase (Roche) (both in DMEM) and 2 d in 200 U ml^{-1} collagenase II (Gibco) and 1 U ml^{-1} papain (Sigma) in CM. All digestion steps were done on a roller at 37 °C and 5% CO_2. After cartilage digestion, the resulting cell suspension was centrifuged at 300 ×*g*, the pellet was resuspended in phosphate-buffered saline (PBS, Gibco) and cells were counted using a CASY1 cell counter (Schärfe Systems). In all, 3 × 10^6 cells were subsequently seeded per T75 flask and cultured in CM at 37 °C and 5% CO_2, changing media twice a week. Cells were passaged when reaching ~90% confluency and cultured until the end of passage one for all experiments.

2.3. Transduction of ASC/TERT1

ASC/TERT1 were transduced to express mCherry for cell tracking as previously described elsewhere [25]. Briefly, Phoenix-Ampho cells were transduced with pBMN vector containing cDNA for the expression of mCherry at 80% confluency using Lipofectamine 2000 (Thermo Fisher). The virus-containing supernatant was mixed with polybrene (Sigma) at a final concentration of 6 μg ml^{-1} and transferred to ASC/TERT1 at 30% confluence and spinoculation at 800 ×*g* was performed for 1 h at RT. Subsequently, the medium was changed to fresh EGM-2, and ASC/TERT1 were cultured to 70% confluence before splitting.

For analysis of F-actin, ASC/TERT1 were transduced with LifeAct-RFP (ASC/TERT1-LA) using rLV-Ubi-LifeAct lentiviral vectors according to manufacturer's protocol (Ibidi). In short, cells were seeded in EGM-2 the day prior to transduction, reaching 30% confluence at the time of transduction. Polybrene at a final concentration of 6 μg ml^{-1} and lentivirus at a MOI of 2 were added, followed by a spinoculation step using 800 ×*g* for 90 min. Cells were cultured in fresh medium for 3 d under standard culture conditions until the RFP signal became visible and were subsequently selected using EGM-2 containing 0.3 μg ml^{-1} puromycin for 1 week. Selected cells were propagated in EGM-2.

2.4. Compartmentation of plates

To generate grid plates, standard 60 mm cell culture-treated Petri dishes (Corning) were laser engraved using a Trotec Speedy 300 (Trotec Ltd) CO_2 laser with a standard wavelength of 10.6 μm, set to a power of 12 W and a pulse frequency of 5000 Hz. The speed was set to 35.5 cm s^{-1} and lines were laser engraved with a 1 or 3 mm offset to the previous line in a grid pattern dependent on desired grid size (supplementary figure 1 (available online at stacks.iop.org/BF/13/035018/mmedia)).

2.5. Size modulation of grid plate spheroids

To investigate the controllability of generated spheroid size via variation of grid sizes, ASC/TERT1 were seeded into grid plates with 1 mm and 3 mm grid size at 1 × 10^6 cells per plate. Cells were cultivated in low-dose differentiation for 3 weeks until spheroid formation was fully concluded. Spheroid size was analysed using Eclipse TE2000-U and NIS-Elements BR 4.20.03 software. For 3 mm grid plates 338 and for spheroids generated by 1 mm grids 800 spheroids were measured for horizontal and vertical diameter. Data were tested for normality using D'Agostino and Pearson omnibus normality test ($p < 0.0001$) and statistical significance of size difference was tested using two-sided Mann–Whitney test.

2.6. Spheroid formation kinetics and effects of ASC/TERT1:hAC ratios

For assessment of spheroid formation kinetics and the effect of ASC/TERT1:hAC co-culture ratios on kinetics and resulting spheroid sizes, ASC/TERT1 alone ($n = 5$), primary hAC alone ($n = 3$) or in co-culture ($n = 5$) were seeded on grid plates with 3 mm grid size at 1 × 10^6 cells/plate. All cultures (ASC/TERT1 mono-cultures and co-cultures) were performed in low-dose differentiation medium, except for pure hAC cultures that were also cultured in CM. Ratios tested for co-culture were 0.8:0.2, 0.5:0.5 and 0.2:0.8 million cells. The number of fully formed spheroids was counted manually twice a week. For the definition of the start point for rapid spheroid formation, a threshold of 25 fully formed

spheroids was used. The time point for the formation of 25 spheroids was calculated by exponential curve fitting ($R^2 > 0.9$) and interpolation. Non-Gaussian distribution was assumed due to small sample size. Spheroid sizes were measured after 5 weeks of culture using TE2000-U and NIS-Elements BR 4.20.03 (Nikon) software, and data was tested for normality using the D'Agostino and Pearson omnibus normality test ($p < 0.0001$). Statistical significance of difference in formation speed and spheroid size was tested using the Kruskal–Wallis and Dunn multiple comparison tests. Additionally, time-lapse imaging of spheroid formation was done using Lumascope 620 and Lumaview software (Etaluma).

2.7. Fibrin embedding of spheroids

To assess the possibility of using grid plate-generated spheroids as organoids to potentially fill defect sites with suitable cartilage, they were embedded into fibrin as a model hydrogel. ASC/TERT1 and 0.5:0.5 million ASC/TERT1:hAC cultures were generated on 3 mm grids. Cultures were kept for 3 weeks prior to harvesting by gentle resuspension using a 1 ml pipette for embedding. Tissucol/Tisseel (fibrinogen: 72–110 mg ml^{-1} + 3000 KIU ml^{-1} aprotinin; thrombin: 500 IU ml^{-1}; Baxter) was used as stock. Thrombin was diluted 1:8 to reduce reaction speed, and fibrinogen was diluted 1:8 with CM containing cell spheroids prior to mixing. Afterwards, the embedded spheroids were cultivated for 2 weeks. Cultures were imaged twice a week and time-lapse imaging of cellular outgrowth spheroids was performed for the first 3 d of culture using Lumascope 620 and Lumaview software.

2.8. (Immuno-)histology

Samples were fixed in 4% neutral buffered formalin overnight at 4 °C and subsequently rinsed with PBS, dehydrated using a graded series of ethanol and, after changing to xylol (Carl Roth), embedded into paraffin. A rotary microtome (MICROM HM355S, Thermo Fisher Scientific) was used to create sections of 3–4 μm thickness for staining. Azan staining was used as the overview staining showing collagen matrix in blue and cells in red. For analysing matrix composition, Alcian blue (0.3% at pH 2.5) for glycosaminoglycans (GAG) with Sirius red counterstaining and immunostaining for collagen type II (Thermo Fisher Scientific, clone 6B3) were used. For analysis of cell division and apoptotic cell death immunostaining for Ki67 (abcam, clone SP6) and cleaved caspase-3 (Cell Signaling, Asp175) were used. For the immunoreaction, alkaline phosphatase and endogenous peroxides were blocked using BIOCALL reagent (Vector Labs). For collagen type II antigens were retrieved by treatment with pepsin (pH 2) and Ki67 as well as cleaved caspase-3 with EDTA buffer (10 mM Tris, 1 mM EDTA, 0.05% Tween 20, pH 9). Samples were incubated with collagen type II (1:100), Ki67 (1:200) or cleaved caspase-3 (1:100) primary antibodies for 1 h at room temperature and subsequently incubated with BrightVision Poly-HRP secondary antibody (VWR). For detection, the NovaRED™ peroxidase substrate kit (Vector Labs) was used. Haematoxylin was used for nuclear counterstaining.

2.9. Comparison of pellet culture to grid plate culture

For standard pellet culture, 96-well round bottom plates were coated with poly(2-hydroxyethyl methacrylate) (poly-HEMA, Sigma). A total of 0.5 g poly-HEMA was dissolved in 95% ethanol overnight at 38 °C while shaking. A total of 50 μl of the solution were added per well and plates were left at 37 °C while shaking to evaporate ethanol for at least 8 h. ASC/TERT1 and ASC/TERT1:hAC (0.5:0.5) pellets were created by seeding a total of 5000 cells per well and centrifuging at 650 $\times g$ for 5 min, yielding pellets of a similar size to grid plates (300–350 μm). Cultures on grid plates were seeded at 1×10^6 cells per plate. Both, well plate (200 μl total media/well, 150 μl media change) and grid plate cultures (4 ml total media/plate, 3 ml media change) were cultivated in low-dose differentiation medium, changing media twice per week. Cell samples before seeding and pellets/spheroids after 3 and 5 weeks of cultivation were taken for qRT-PCR ($n = 4$, 12 pellets/spheroids per n) and (immuno-)histochemistry ($n = 4$, 12 pellets/-spheroids per n).

2.10. Image quantification

Histological sections were quantified using the Fiji distribution of ImageJ [26]. Collagen type II and GAG were quantified by mean intensity analysis for the spheroid area ($n = 4$ experiments). For collagen type II also outer (~60% of area) and inner area (~40% of area) were measured separately (a visual representation of the regions of interest (ROI) can be found in supplementary figure 6). Spheroids with strong focal collagen type II staining for different ASC/TERT1:HAC ratios, and Ki67 and cleaved caspase-3 positive cells per spheroid were counted using the multipoint tool. Circularity and roundness were analysed via the corresponding parameters in the measurement tool. Filament orientations in compartment corner regions were analysed using the OrientationJ plugin using the visual directional analysis [27], distribution of orientation ($n = 4$) [28] and quantitative orientation measurement ($n = 7$) [29] tools. Cortex thickness was measured in confocal images of five grid plate spheroids and five pellets from standard pellet culture from ASC/TERT1-LA mono-cultures in three areas per spheroid/pellet.

Cellular outgrowth from fibrin embedded spheroids was measured as radius from the centre point and subsequently normalised to the initial radius of the spheroid at d0 in horizontal and vertical orientation, and for ASC/TERT1 d14 in the directions

of enhanced directional and standard outgrowth. Illustrations of the measurement can be found in supplementary figure 11. All quantified data were tested for normal distribution using Shapiro–Wilk test (when n-number was sufficient). For comparison of two groups unpaired t-test or Mann–Whitney test and for comparison of multiple groups one-way ANOVA with Holm–Sidak's multiple comparison test or Kruskal–Wallis test with Dunn's multiple comparison test were chosen according to distribution.

2.11. Life/dead staining

For analysis of cell viability and cell death in ASC/TERT1 mono- and co-culture with hAC in grid plates and standard pellet culture spheroids/pellets were stained using LIVE/DEAD viability/cytotoxicity kit for mammalian cells (Invitrogen) according to supplier instructions. In short, spheroids/pellets were harvested and washed in PBS before being stained with 2 μM calcein-AM and 4 μM Ethidium homodimer-1 for 15 min at 37 °C and were immediately imaged.

2.12. mRNA isolation and qRT-PCR

Spheroids were lysed in RLT lysis buffer containing 10 μl ml^{-1} β-mercaptoethanol, frozen and kept at −80 °C until further processing. RNA was isolated using the RNeasy Micro Kit (Qiagen) according to the manufacturer's protocol, eluting with 14 μl UltraPure DEPC-treated water (Invitrogen). RNA concentrations were measured using a NanoDrop 2000c spectrophotometer (Thermo Scientific). RNA samples were subsequently reverse transcribed using iScript cDNA synthesis kits (Bio-Rad) according to the manufacturer's protocol using a Primus 25 thermal cycler (MWG Biotech). qPCR was performed using the SensiMix II probe kit and TaqMan probes (20 μl reactions) for Col1a1 (Col1, Applied Biosystems, Hs00164004 m1), Col2a1 (Col2, Eurogentec, forward: 5′-GCC-TGG-TGT-CAT-GGG-TTT-3′, reverse: 5′-GTC-CCT-TCT-CAC-CAG-CTT-TG-3′, probe: 5′-AAA-GGT-GCC-AAC-GGT-GAG-CCT-3′), aggrecan (ACAN, Applied Biosystems, Hs00153936_m1) and HPRT1 (Applied Biosystems, Hs02800695_m1) as housekeeping gene on a 7500 Fast Real-Time PCR system (Applied Biosystems). Data was analysed using ΔΔCT-method, normalising Col1 and Col2 expression to ASC at d0 of experiments. ACAN was normalised to HAC at d0 of experiment as no ACAN expression was detectable in ASC at d0. Statistical analysis was done using Kruskal–Wallis test with Dunn's multiple comparison test.

2.13. Statistical analysis

All statistical tests were done using GraphPad Prism 6.01, as described in the respective paragraphs above. Groups were considered significantly different with an α-value < 5% ($p < 0.05$). Box and whisker plots are given with whiskers for 1st and 99th percentiles, and non-histogram bar charts are given as mean ± standard deviation.

3. Results

Spheroid formation was observed on compartmented culture dishes of 6 cm diameter, generating one spheroid per compartment and yielding a total of approximately 200 spheroids per dish. The assessment of the formation process revealed distinct phases with progression from monolayer to fully formed spheroids (figure 1). Co-cultures showed a big impact on the system and led to an increased formation speed of spheroids. When comparing the grid plate system to standard pellet culture, a similar differentiation capacity could be achieved, with less variation than in the standard pellet culture setup. Finally, embedding the spheroid into fibrin hydrogel showed cellular outgrowth and matrix deposition into the gel.

3.1. Cells self-assemble into spheroids on compartmented growth surface

In order to test the behaviour of two different cell types with chondrogenic potential on the grid plates, hAC and ASC/TERT1 were seeded in compartmented cell culture dishes (1×10^6 cells per 6 cm Petri dish; 1 mm and 3 mm grid size) and cultivated in proliferation and low chondrogenic differentiation medium (containing a low dose of growth factor), respectively. Both cell types did not adhere to the laser incisions, but only to the compartment surface where they initially formed a standard 2D monolayer (figure 1). With increasing confluence, cells started to aggregate and form spheroids. The much faster proliferating ASC/TERT1 took approximately 3 weeks until spheroids were free-floating in the medium (figure 1), while chondrocytes reached this state after 2 months or longer (supplementary figure 3). The final size of spheroids was controllable by the grid size resulting in ASC/TERT1 spheroids with significantly different mean diameters of 134 μm and 340 μm for 1 mm and 3 mm grid size, respectively ($p < 0.0001$; supplementary figure 2). Due to the faster formation speed, ASC/TERT1 were used to more closely assess the assembling process of grid plate-induced spheroids by observation in regular intervals (figure 1) and via time-lapse imaging (supplementary video 1: spheroid formation). Three millimetre grid size was chosen for comparison with standard pellet culture, as standard pellet culture becomes increasingly impractical with decreasing pellet size. After the monolayer phase, the spheroid formation phase started with a slight contraction and condensation of the cell layer in the periphery of the compartments, which was most pronounced in the corners (figure 1(a), day 12). This was followed by rolling up of the cell layer (figure 1(a), day 25), which typically happens in an elongated cell bulge at the cell layer front. At the end of this rolling

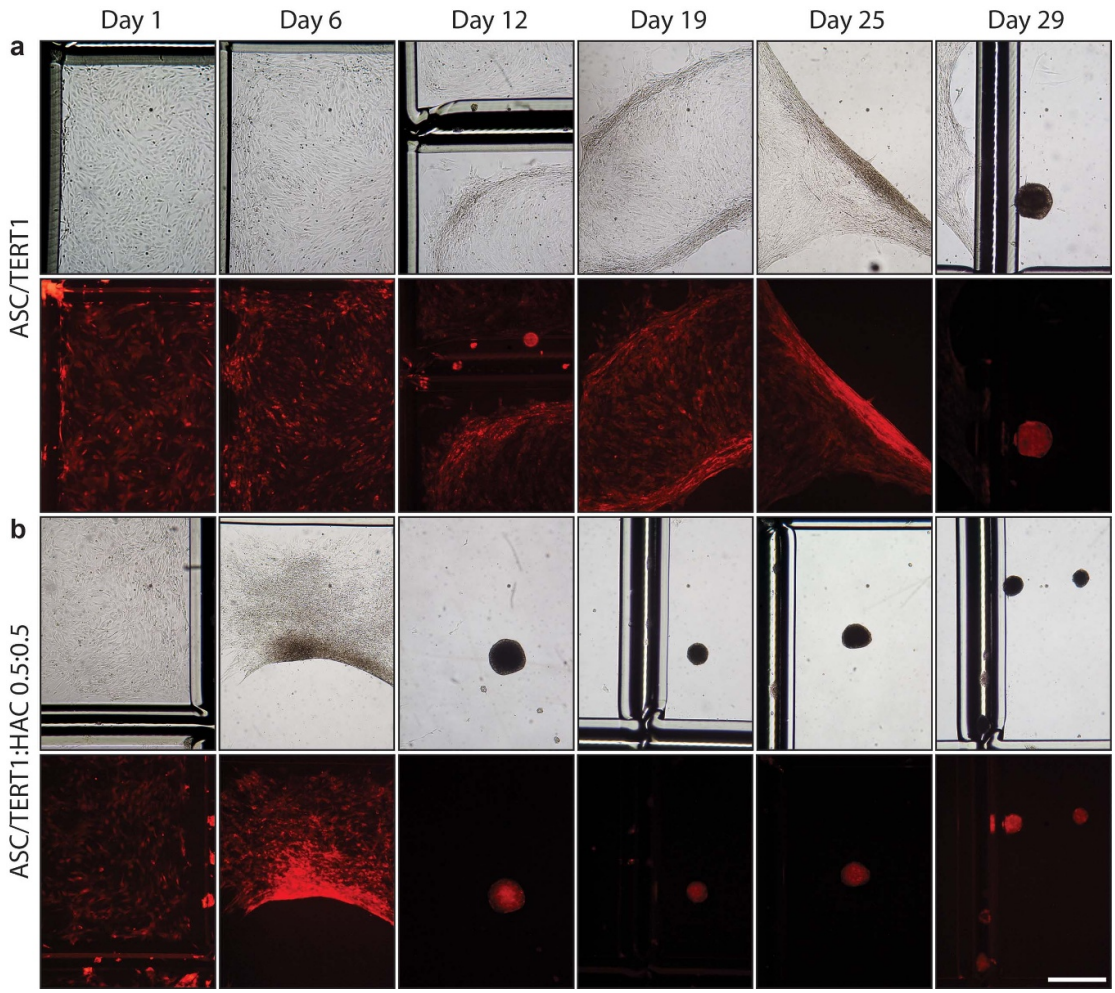

Figure 1. Bright-field and fluorescence imaging of spheroid formation for (a) ASC/TERT1 and (b) 0.5:0.5 ASC/TERT1:hAC co-culture on a 3 mm grid plate over a period of 29 d. (a) In ASC/TERT1 mono-culture starting spheroid formation could be observed after about 2 weeks, with spheroids being fully formed after 3–4 weeks. (b) Co-cultures showed starting spheroid formation within 1 week and completed spheroid formation within 2 weeks (μ-bar = 500 μm).

up stage, usually 2–3 anchor points to the plate surface were left. Subsequent conversion into spheroid form happened rapidly within 30–60 min by loss of an anchor point and contraction into a knob-like structure. In the final stage of spheroid formation, spheroids condensed fully to take on a spherical shape (figure 1(a), day 29).

To gain more insight into the contraction of the cell monolayer, ASC/TERT1-LA with red fluorescent actin filaments were used for spheroid formation and imaged by confocal microscopy (figure 2). Cells in the periphery of the compartments aligned along their edges exhibiting a well-developed actin cytoskeleton (figure 2(a)). In the corners, further cells with high amounts of oriented actin cytoskeleton aligned radially to the centre (figure 2(b)). This was clearly visible when analysing filament orientation (figures 2(e)–(h), supplementary figure 4) showing peaks at 0°, 45° and 90° corresponding to the border regions and the intermediate area. Additional peaks were observed at −45° and 145° resulting from cells that change direction between the other alignments. When cell layers began to roll-up, actin was aligned along the roll-up front. Cells beside and fusing with the roll-up region exhibited actin alignment perpendicular to the roll-up front (figure 2(c)). In fully formed spheroids, only the cortex region displayed a thin layer of cells with strongly aligned actin filaments, while the central areas revealed random F-actin alignment (figure 2(d)).

3.2. Co-culture of ASC/TERT1 and hAC accelerates the self-assembling process

As ASC/TERT1 formed spheroids faster than hAC, it was tested if the addition of ASC/TERT1 to hAC cultures could speed up the formation process compared to hAC mono-cultures. Surprisingly, the co-cultures proved to be even faster in forming spheroids than ASC/TERT1 mono-culture (figure 1(b)). As ASC/TERT1 and co-cultures, in contrast to initial hAC mono-cultures, were tested in low-dose differentiation medium, hAC mono-cultures were also tested

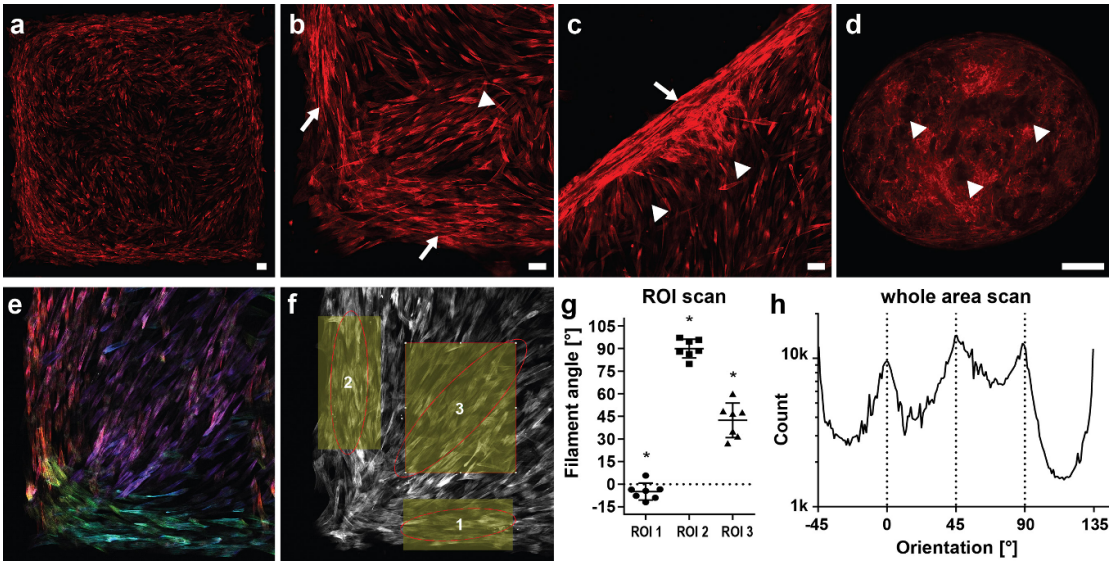

Figure 2. Confocal imaging of F-actin orientation during spheroid formation in ASC/TERT1-LA. (a) Overview of one compartment with condensation starting at the border. (b) Corner region of the compartment while starting contraction showing actin aligned along the compartment borders (arrows) and radially to the centre (arrowhead). (c) Monolayer beginning to roll-up (arrow) with cells exhibiting actin aligned perpendicular to rolled up zone (arrowheads) and (d) fully formed spheroid with cell free voids formed by matrix sheets (arrowheads) (μ-bar = 100 μm). (e) Orientation map of the corner region showing 0° in turcoise, 45° in purple and 90° in red. (f) Measurement areas for horizontal border region (ROI 1), vertical border region (ROI 2) and intermediate area (ROI 3) and (g) quantification of these areas ($n = 7$). (h) Histogram of mean angle distribution in the corner areas as in (e) ($n = 4$), showing maxima at 0°, 45° and 90° as well as −45° and 135° corresponding to cells in the very tip of the corner (green in (e)).

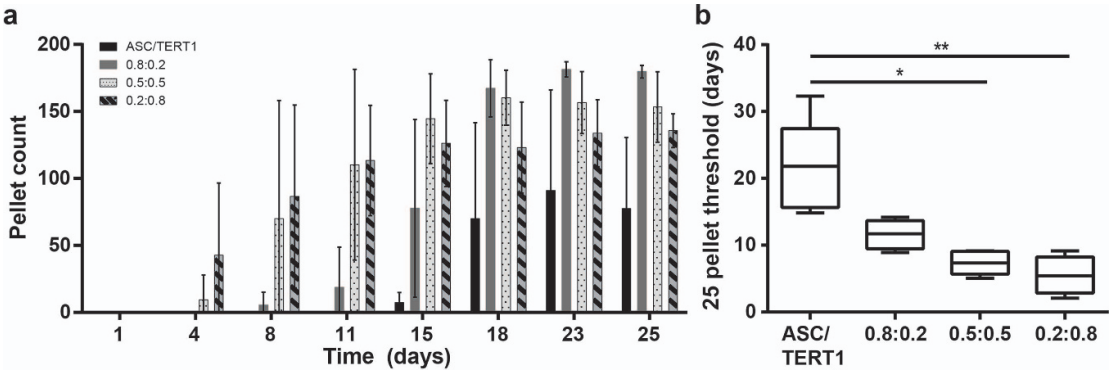

Figure 3. Spheroid formation speed of ASC/TERT1 or co-culture (ratio ASC/TERT1:hAC) on grid plates. (a) Spheroid count over a period of 25 d showing a faster spheroid formation rate in cultures with increasing hAC ratio. (b) Duration of reaching a spheroid count threshold of 25 was selected as a start point. $^{*}p < 0.05$; $^{**}p < 0.01$.

in this medium. However, they assembled into very small spheroids without prior formation of a stable cell layer.

In order to assess the kinetics of spheroid self-assembly and to more closely look at the effect of co-culture, fully formed spheroids of ASC/TERT1 mono-culture and different co-culture ratios (ASC/TERT1:hAC ratios: 0.8:0.2, 0.5:0.5 and 0.2:0.8) were assessed over 3.5 weeks (figure 3(a)). The comparison of the counts of readily formed spheroids revealed that co-culture spheroid formation was cell ratio-dependent, starting formation about 1 week sooner than ASC/TERT1 spheroids (21 ± 7 d), and due to similar kinetics during formation, also completed spheroid formation significantly earlier. Co-cultures with 0.5:0.5 and 0.2:0.8 ASC/TERT1:hAC were shown to form spheroids significantly faster (7 ± 2 d and 6 ± 3 d, respectively) than pure ASC/TERT1 cultures (figure 3(b), $p < 0.05$ and $p < 0.01$, respectively). The 0.8:0.2 ASC/TERT1:hAC cultures were not significant, but they still showed a trend to be slightly faster (12 ± 2 d) in spheroid formation than ASC/TERT1 cultures.

3.3. Spheroid parameters can be influenced by ratio of ASC/TERT1 and hAC

Since acceleration of spheroid formation in co-cultures was observed, the effects of co-culture ratios on spheroid sizes were investigated (figure 4). Mean sizes ranged from 308 μm to 150 μm in

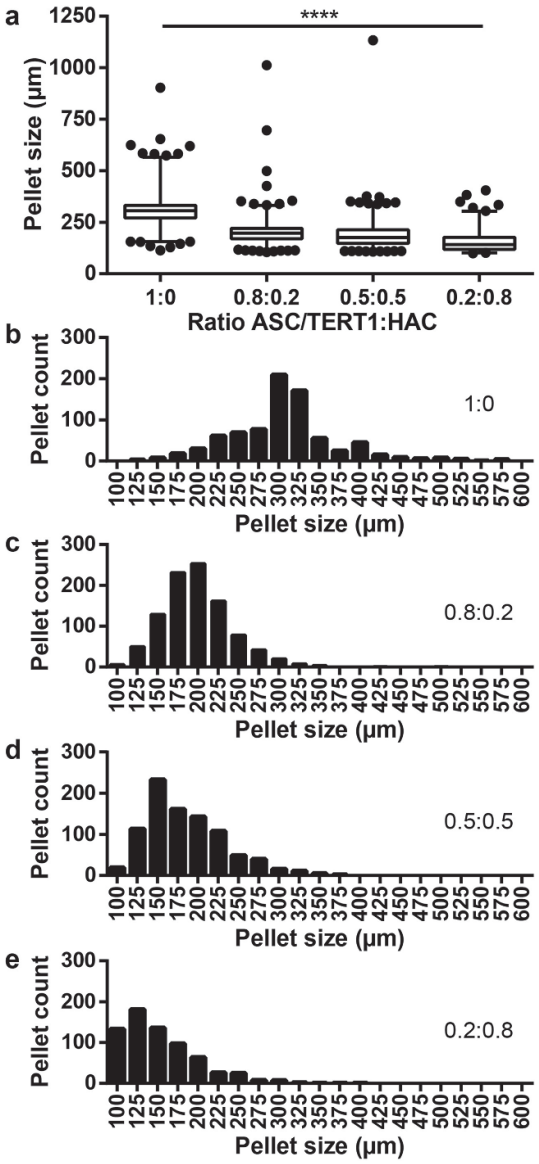

Figure 4. Effect of ASC:hAC ratio on resulting spheroid size for 3 mm grid plates. (a) Histogram of spheroid size distribution for different ASC/TERT1:hAC ratios, (b) ASC/TERT1 only, (c) 0.8:0.2, (d) 0.5:0.5 and (e) 0.2:0.8, showing a shift to smaller spheroid sizes with increasing hAC ratio. $^{****}p < 0.0001$.

ASC/TERT1 only and 0.2:0.8 ASC/TERT1:hAC cultures, respectively. The most common spheroid size (within a ± 12.5 μm range) per group was: 300 μm (ASC/TERT1), 200 μm (0.8:0.2), 150 μm (0.5:0.5) and 125 μm (0.2:0.8). Size differences were statistically significant in all conditions ($p < 0.0001$). Due to the earlier spheroid formation, with higher hAC ratios (0.2:0.8), the size became more variable, with increasing numbers of small spheroids. The total number of spheroids was therefore higher, but were not counted as they fell below the threshold size of 100 μm. Additionally, in most conditions, individual very large spheroids could be observed, which formed via not fully compartmented areas in the outermost regions of some plates.

Histology revealed different internal spheroid structures in the four cell-type ratios (figure 5). ASC/TERT1 cultures showed large regions with thick matrix strands, while co-culture spheroids exhibited a more homogenous appearance of deposited matrix. In accordance with the size measurements, increasing percentages of hAC showed higher numbers of small spheroids. Furthermore, they contain intense spots of collagen type 2 labelling more frequently than ASC/TERT1 mono-culture (despite not being statistically significant, supplementary figure 5). According to the more regular size and internal structure, the 0.5:0.5 ASC/TERT1:hAC ratio was used as co-culture conditions for subsequent experiments, yielding the best compromise between formation speed and system stability. Also, in non-compartmented dishes, monolayer 0.5:0.5 ASC/TERT1:hAC co-cultures (figure 5, 0.5:0.5 unstr.) rolled up, even though after a very long generation time ($\sim$2 months). The resulting singular spheroid showed similar strand-like matrix structures as in ASC/TERT1 spheroids. The matrix was arranged in regular layers between cell dense sheets, appearing as spiral patterns at the perpendicular section plane, with the innermost layer being formed by cells. This structure likely occurs due to matrix deposition during prolonged 2D phase and subsequent rolling up of the cell layer with simultaneous incorporation of the matrix layers.

3.4. Grid plate spheroids have comparable differentiation capacity as standard pellets

To compare the differentiation capacity of grid plate spheroids with standard pellet culture, ASC/TERT1 only and 0.5:0.5 co-culture were analysed after 3 weeks, as well as 5 weeks of culture using qRT-PCR. To eliminate influences from varying spheroid/pellet sizes and cell numbers between grid plate spheroids and pellets, cell number dilution series were performed in standard pellet culture, yielding comparable pellet sizes to 3 mm grid plates when using 5000 cells/well. Col1 expression levels showed no significant differences between cell-type ratios and time points (figure 6(a)). Also, Col2 expression was similar between grid plate spheroids and standard pellets and did not show any significant difference within the same cell-type ratio, but trended to slightly higher expression levels in standard pellets (figure 6(b)). Despite Col2 expression not reaching significant difference between 3 and 5 weeks, and between ASC/TERT1 and co-culture, a positive trend was visible. The differentiation index (Col2/Col1) reflected these findings; however, standard pellet culture showed much higher variability, especially in co-cultures, where grid spheroids yielded more reproducible results (figure 6(c)). ACAN expression (figure 6(d)) corresponds with the results found for Col2 and differentiation index, while showing even lower differences between grid and standard pellet

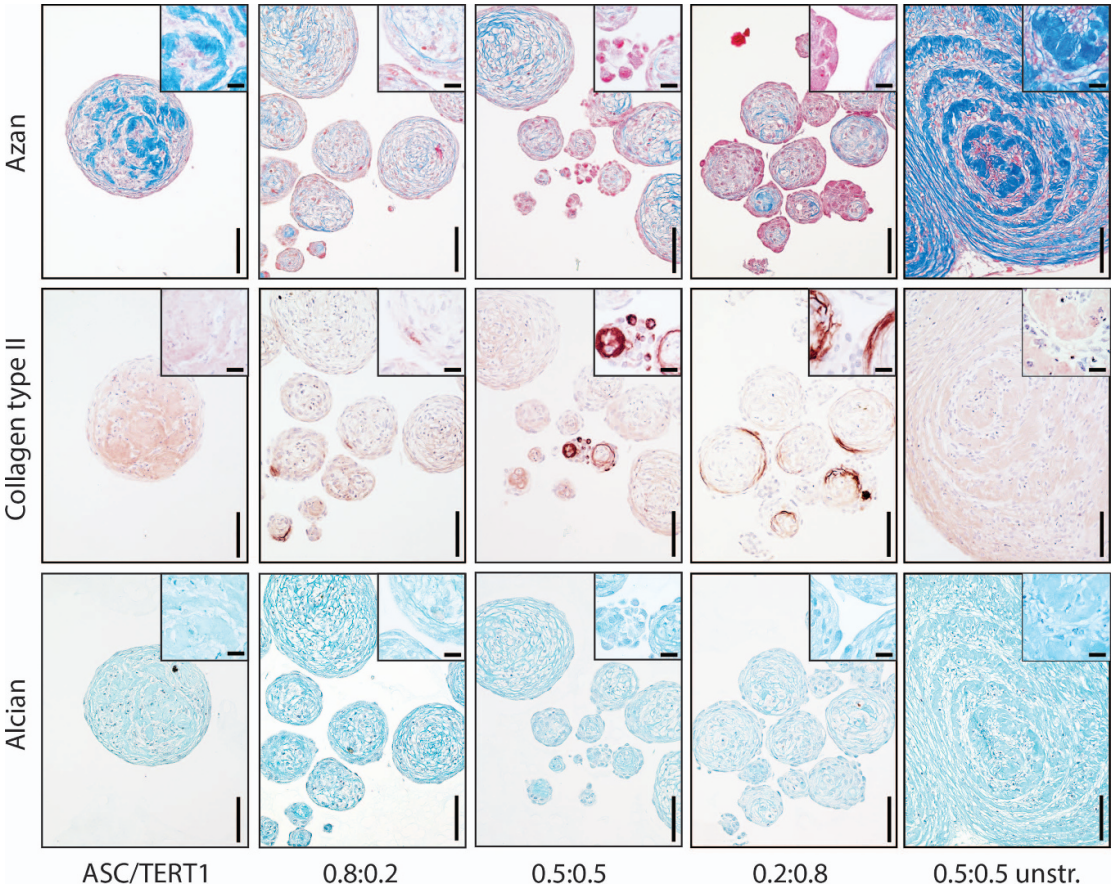

Figure 5. Histological sections of different ASC/TERT1:hAC ratio spheroids grown on 3 mm grid plates (after 5 weeks of culture) and not compartmented plates (0.5:0.5 unstr., after finished formation of ∼2 months), stained for ECM formation (Azan), collagen type II and GAG (Alcian). Azan staining showed differences in matrix distribution, with conditions leading to longer 2D phase (ASC/TERT1 mono-culture and unstructured plates), showing increased matrix dense regions, while other conditions led to a more dispersed matrix distribution. Increase in the ratio of hAC (0.8:0.2–0.2:0.8) showed an increased amount of small size spheroids and an increase of zones with high collagen type II expression. (μ-bar = 100 μm; μ-bar inserts = 20 μm).

culture. However, ACAN expression showed a significant difference between ASC/TERT1 only and co-culture for standard pellets after 5 weeks of culture ($p < 0{,}05$; 15-fold increase), while other conditions showed a positive trend in co-cultures.

Histological analysis (figure 6(e)) and quantification of staining intensity (collagen type II and GAG supplementary figure 6) reflected the results seen in qRT-PCR. Between grid plate spheroids and pellets no difference was observed in ASC/TERT1 culture. In co-cultures, only a slight but statistically not significantly higher intensity was visible in pellets in comparison to spheroids. Comparing the two different cell-type groups, co-cultures in general showed a trend to higher staining intensity than ACS/TERT1 mono-culture. However, statistical differences were only found between some of ASC/TERT1 mono- versus co-cultures (GAG at week 3 and collagen type II at week 5).

When assessing the collagen type II distribution between cortex and centre area (cortex-centre index; supplementary figure 6), grid plate spheroids trended to a more even distribution than standard pellets with a ratio of 1–1.1. Only in 5 week co-cultures a higher cortex-centre ratio was measured in individual cases (mean ratio of 1.3, individual spheroids up to a ratio of 1.9). In contrast, pellet culture generally had a trend to exhibiting slightly higher collagen II intensities in the cortex compared to the inner area (mean ratio of 1.2–1.4). However, a significant difference between grid and pellet culture was only found for ASC/TERT1 cultures at week 3. In addition to histology, fluorescence images revealed the differences between cortex and centre on a cellular level. The alignment of ASC/TERT1-LA in the cortex region (figure 6(f)), which was significantly thicker in pellets (mean 47.5 μm) than in grid plate spheroids (mean 27.0 μm) (supplementary figure 10), was clearly observable. The alignment of the cells in the cortex led to the adaptation of a more elongated cell morphology.

3.5. Grid plates exhibit comparable circularity to standard pellet culture

Circularity and roundness of spheroids were comparable between both culture systems (grid plates and pellet culture) with mean circularity above 0.95 for all conditions and mean roundness between 0.95

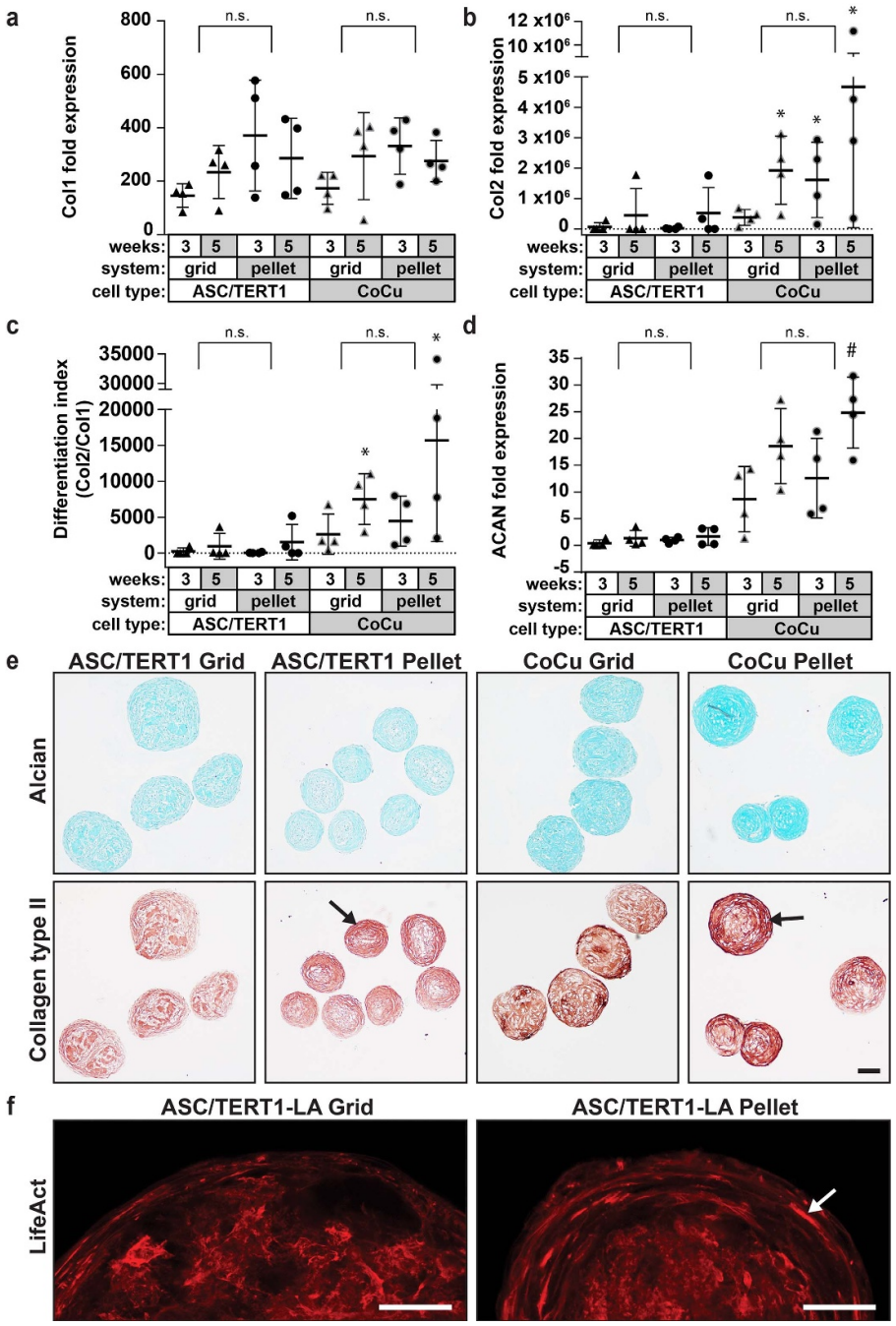

Figure 6. Comparison of grid plate spheroids and standard pellet cultures. Fold gene expression of (a) Col1, (b) Col2, (c) differentiation index (Col2/Col1), and (d) ACAN of ASC/TERT1 only and 0.5:0.5 co-cultures generated in grid plates and standard pellet cultures normalised to ASC at seeding (ACAN was normalised to hAC at seeding as it was not detectable in ASC at seeding). Relative gene expression and differentiation index showed no significant difference between grid plate and standard pellet culture but higher Col2 expression in co-culture versus ASC/TERT1 mono-culture. (d) (Immuno-)histochemistry of ASC/TERT1 only and 0.5:0.5 co-cultures from grid plates and standard pellet cultures stained for GAG (Alcian) and collagen type II. Spheroids from grid plates and pellets from standard pellet cultures showed comparable staining; however, they both showed differences in internal structure. Pellets showed a thick strongly aligned cortex (arrows) that was not present in grid plate cultures, which exhibited strands of dense matrix. Co-cultures showed regions of especially high collagen type II staining, indicating high local numbers of chondrocytes (μ-bar = 100 μm). (e) Confocal imaging of ASC/TERT1-LA visualising F-actin orientation, showing a thicker aligned cortex region (arrow) in ASC/TERT1-LA pellet cultures than in grid plate cultures (μ-bar = 50 μm). $^*p < 0.05$ compared to d0; $\#p < 0.05$ ASC compared to the corresponding co-culture.

and 0.85 for all conditions (supplementary figure 7). Slightly lower circularity was only found for grid cultures with ASC/TERT1 at 5 weeks and co-culture at 3 weeks. However, a significant difference could only be seen between two groups (ASC/TERT1 5 weeks, co-culture 3 weeks) and grid co-cultures after 5 weeks, which exhibited the highest circularity values of all conditions. The same was visible in roundness, where another group (co-culture pellets 3 weeks) significantly differed from grid co-cultures after 5 weeks.

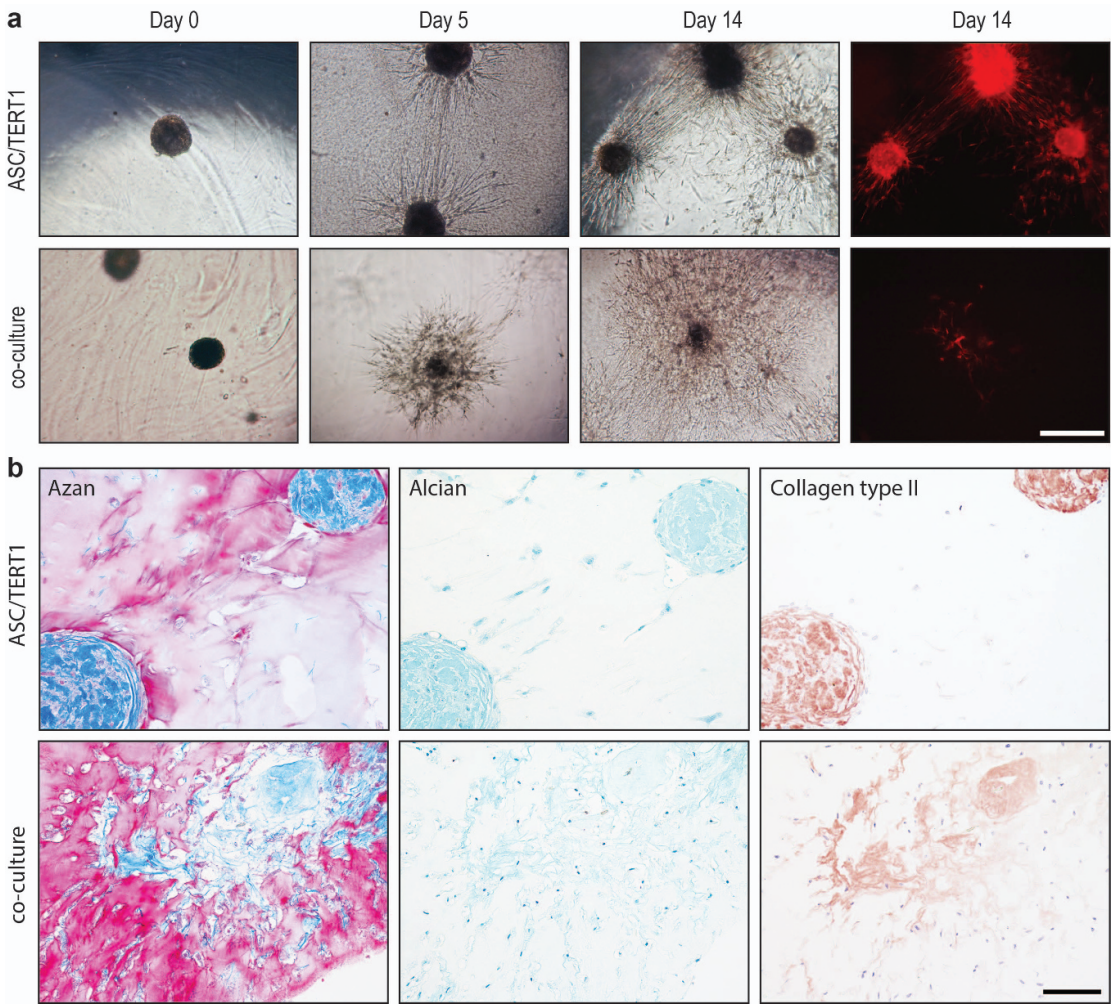

Figure 7. Cellular outgrowth behaviour of ASC/TERT1 spheroids and 0.5:0.5 ASC/TERT1:hAC spheroids generated on grid plates and embedded into a loose formulation of fibrin. (a) Bright-field images of days 0, 5 and 14, and fluorescence (red = mCherry labelled ASC/TERT1) image of day 14 after embedding. Both types of culture exhibit cellular outgrowth behaviour; however, it is much more pronounced in co-culture. (b) Histological sections stained for structural discrimination of cells, matrix and fibrin gel (Azan) for GAG (Alcian) and collagen type II showing stronger matrix deposition in co-cultures (μ-bar bright-field/fluorescence = 500 μm; μ-bar histology = 100 μm).

3.6. Grid plate-generated spheroids show similar cell turn-over compared to standard pellet culture

To assess the viability of grid spheroids and compare the cell turn-over to standard pellet culture, life/dead staining was performed showing strong calcein-AM staining and only few dead cells, visualised with staining of nuclei by ethidium homodimer-1 (supplementary figure 9). Also, staining for Ki67 and cleaved caspase-3 showed only few positive cells (supplementary figure 8). Grid plate culture had slightly more Ki67 positive cells, however there was no significant difference. For cleaved caspase-3 ASC/TERT1 cultures showed slightly higher values than co-cultures, but again no significant difference could be observed.

3.7. Grid plate-generated spheroids are able to populate hydrogels in a cell type-specific manner

To test the repopulation and matrix deposition into hydrogels by grid plate-generated spheroids used as pre-differentiated organoids for regenerative medicine applications, ASC/TERT1 and 0.5:0.5 hAC:ASC/TERT1 co-culture spheroids were embedded into a loose formulation of a fibrin gel ($\sim$11 mg ml^{-1}). Both mono- and co-cultures showed significant (vs. d0) cellular outgrowth (figure 7(a); supplementary figure 11(a)), which was not significantly different between mono- and co-cultures when looking at outgrowth radius. However, co-cultures showed equally strong outgrowth in all directions (figure 7(a)), leaving almost no central cores and reaching an approximate outgrowth radius of 0.5 mm after 14 d. In contrast, ASC/TERT1 spheroids showed significantly higher mean cellular outgrowth radius in the direction of other spheroids (573 μm) compared to general outgrowth (232 μm) (supplementary figure 11(c)), while the main part of the spheroid persisted for the time of observation (14 d). The different outgrowth behaviour was documented using time-lapse imaging

(supplementary video 2: spheroid cellular outgrowth). (Immuno-)histochemistry staining revealed that ASC/TERT1 deposited only very little matrix around the spheroids, while the co-cultures exhibited clear deposition of GAG and collagen type II into the fibrin matrix.

3.8. Grid plates allow for a significant reduction in used media

To estimate the reduction in media use possible with the grid plate system (3 ml/dish) compared to pellet culture using 96-well plates (150 μl/well), media used per media change was calculated. At 200 spheroids (produced by one grid plate) a 10× reduction in media use can be achieved with the grid plate system. The break-even point was calculated for 20 spheroids (supplementary figure 12). Due to the flexible process of grid plate production derivates, using other cell culture vessels as starting material, can easily be produced (e.g. using 6-well or 12-well plates, supplementary figure 1). Six-well and 12-well plates reduce the break-even point to 9 and 4 spheroids, respectively, while allowing for the production of 89 and 32 spheroids per well, respectively (supplementary table 1). When increasing the amount of spheroids generated, this grid well plate systems show a stepwise increase in used media, always staying far below the media used in 96-well plates (supplementary figure 12).

4. Discussion

In this study, an easy manufacturing system for micromass spheroids is presented, functioning via induction of autonomous spheroid formation from monolayer via growth surface compartmentation. This allows for a considerable reduction of handling time and reagent usage. Additionally, due to the characteristics of the spheroid formation process, early readout parameters might be gained. The process of spheroid formation could be divided into three phases: initial edge contraction, followed by condensation, leading to roll-up and spheroid formation. Two main factors seem to drive this self-assembly into micromass spheroids: (a) the contractile force of the cells themselves and (b) detachment of the cell layer from the substrate. (a) The influence of the forces within a cell layer previously predicted by a mechanical stress model [30] agrees with the F-actin orientation (alignment with compartment borders and radial alignment in the corner regions) and starting points of condensation (high mechanical stress regions in corners) observed in this study. In previous studies, it was demonstrated that this functional formation of actin filaments, and the subsequent facilitated force transmission, is essential for initial self-assembly into microtissues [31]. The forces generated by dedifferentiated chondrocytes were shown to be strong enough to deform scaffolds [32] and to have an effect on the formation and alignment of extracellular matrix [33], which explains the matrix sheets observed in this study, and which was especially pronounced in ASC mono-culture derived spheroids. In contrast, in fully formed spheroids, increasing matrix deposition and separation of the cells from each other was associated with reduced and randomly aligned F-actin. This shows the change in contractility and suggests chondrogenic differentiation, which was shown to be associated with disruption of the cytoskeletal contractile machinery in chondrocytes [34]. (b) For the detachment from the contracting cell layer, cellular adhesion to the culture surface must be overcome. Cellular attachment to culture plastic and other cells can be strongly influenced by media components, such as serum, and changes in expression of adhesive molecules. Serum replacement was shown to lead to reduced attachment to cell culture plastic [35], which was likely facilitated by the lack of fibronectin and other serum components promoting cell attachment. This also became apparent in the grid plate system, as hAC cultured in serum-rich CM attached relatively strongly to the substrate and only detached over a long duration, while hAC in serum-free medium detached very fast. While media composition seems to play an important role, cell-specific factors also seem to impact the detachment process, as this process is more gradual in ASC and co-cultures than in pure chondrocyte mono-cultures. Alteration of adhesion molecule expression levels or switching to different types was shown during phases of development (e.g. NCAM) [36] and during differentiation in monolayer/3D culture [37, 38]. Furthermore, the importance of cellular adhesion molecules, for interaction with substrate/extracellular matrix (ECM) and force distribution, has been presented (e.g. cadherins) [39]. Thus, during spheroid assembly in the grid plate, a change in attachment to the plate substrate and a switch to stronger cell–cell adhesion or adhesion to the cell-derived matrix could promote spheroid formation. However, detachment as a result of the cellular force and contraction could also be sufficient.

To compare the differentiation capacity of spheroids generated by grid plate culture and standard pellet mono-culture and 0.5:0.5 co-culture, gene expression was analysed. Col1 expression remained stable in all conditions. Col2 and ACAN expression between the grid plate and standard pellet culture was comparable, with a slight trend to higher differentiation in standard pellet culture. This is promising as the immortalised ASC/TERT1 have a higher proliferation rate than primary hAC and proliferated more during the initial 2D phase in grid plates. Consequently, the ASC/TERT1:hAC ratio in the final grid plate spheroids was higher than initially seeded, which differs from standard pellet culture where pellets form immediately. In both, grid plate cultures and pellet cultures, Col2 expression

was significantly increased in co-cultures. This is in accordance with the literature reporting that co-cultures of mesenchymal stem cells and chondrocytes [40, 41] or dedifferentiated and differentiated chondrocytes [42, 43] have positive effects on hAC and mesenchymal stem cells, such as improved chondrogenesis [44, 45], proliferation [41] and suppression of hypertrophy [46]. Underlying mechanisms are either paracrine stimulation via upregulation of growth factor secretion (e.g. TGF-β1) [44, 47–50], or direct cell-to-cell contact [40]. It was shown that these positive effects already occur with amounts as low as 20% of hAC co-cultured with MSC [44] or freshly isolated hAC [43]. The differentiation index reflected the results found in Col2 expression. However, standard pellet culture showed very high variability in co-cultures, while grid plate spheroids produced more reproducible results. The higher consistency within the grid plate system can partly be explained by the cultivation of all spheroids in one culture vessel, allowing for more homogenous auto-/paracrine stimulation than in 96-well plates with completely independent compartments. Thus, inhomogeneous chondrocyte populations (e.g. articular chondrocytes from different zones of native cartilage) or ASC sub-populations can be better equalised, leading to more stable and reproducible results. Additionally, due to the decrease in total media volume these auto-/paracrine factors are likely to be more concentrated, thereby increasing their effectiveness [51, 52].

Histological analysis of GAG and collagen type II reflected the qRT-PCR results, showing that Col2 expression was generally very similar between the two culture systems. In co-cultures, pellets had a trend to slightly higher collagen type II expression. However, grid plate cultures showed a more equal distribution of collagen type II between the cortex and the inner area. This might result from the different development in both systems, starting with a 2D phase in spheroids followed by a later rolling up, while pellets grow by internal matrix deposition and superficial proliferation, also visible by Ki67 staining in the outer pellet region. Co-cultures exhibited an increased number of spheroids containing strongly stained focal regions, indicating a locally high concentration of chondrocytes. Co-culture was also influenced by the cell ratio. Higher hAC ratios led to decreased spheroid size, due to their accelerating effect on rolling up not allowing for complete monolayer formation in ratios higher than 50:50. Cell death as possible explanation for a reduced spheroid size can be excluded, since life/dead staining showed good viability and only low amounts of cell death, also confirmed by a neglectable amount of apoptotic cells stained with cleaved caspase-3. When comparing the internal structure of grid plate spheroids and standard pellet cultures, differences in their internal structure are clearly apparent. Grid plate ASC/TERT1 monocultures especially exhibited internal strands of dense matrix that were likely formed during the monolayer phase between the cell layer and growth surface, as has been previously shown for cell sheets generated on thermo-responsive poly(N-isopropylacrylamide) surfaces [53, 54]. These compact matrix strands might provide a denser and more cartilage-like matrix environment for the cells but also a higher mechanical stiffness which could be an advantage for *in vivo* application. Another difference between grid plate and pellet culture was the structure of the cortex region. While grid spheroids only showed a very thin aligned layer on the surface, pellets showed a significantly thicker layer of aligned cells and matrix. This might limit the necessary rearrangement after *in vivo* application and outgrowth or spheroid fusion into bigger constructs, which was previously shown for micropellets cultured for longer durations [21]. Especially biofabrication approaches require spheroids of constant size and shape. Grid-plate derived spheroids revealed a high regularity with mean circularity and roundness above 0.95 and 0.85, respectively, for all conditions and were comparable between all conditions indicating a very circular overall shape. These values are also in line with other systems for spheroid generation showing mean circularity values of around 0.9 [55, 56]. One reason for occasionally observed reduced circularity of grid plate spheroids is the seldomly occurring agglomeration of spheroids from neighbouring compartments, either because of fusion or incomplete compartmentation. Nevertheless, also standard pellet cultures in some cases show a reduced circularity which can be attributed to the incorporation of small, separately forming, side pellets or focal outgrowth and differentiation, which was visible in co-cultures of both systems.

Due to promising results of grid plate spheroids in terms of differentiation and architecture, the feasibility to use them in 3D *in vitro* models of hydrogel-augmented organoid therapy for regenerative medicine was assessed. Spheroids have previously shown to be promising alternatives to single cells for cartilage tissue repair, especially due to a higher differentiation potential [57–59]. Here, it was shown that, while ASC/TERT1 and co-culture spheroids both showed outgrowth of cells into fibrin hydrogel, co-cultures exhibited more even migration into the gel, spreading into an area comparable with the cartilage thickness (1.3 mm) within 2 weeks. ASC/TERT1 spheroids showed similar or even faster outgrowth in the direction of other spheroids but had much slower outgrowth in other directions. Furthermore, the co-cultures deposited remarkably more matrix, which was collagen type II positive, indicating that cells retained their chondrogenic phenotype. The extensive outgrowth with simultaneous retention of the differentiated state (regained during grid plate culture) is a good indication for their applicability in cartilage regeneration to entirely fill a defect from the spheroids as the initiation centre. For the use

in bioprinting, depending on nozzle size, the use of smaller diameter spheroids might be beneficial. Due to the controllability of spheroid diameter via variation of grid size spheroids, with a mean diameter of 134 μm could be produced when using 1 mm grid size. This is in a similar size range of spheroids previously used for cartilage bioprinting by de Moor *et al* which used spheroids with a mean diameter of 116 μm [56]. The use of spheroids for bioprinting might be beneficial compared to single cell applications due to a better protection against external factors (e.g. shear forces, radicals), facilitated by the associated matrix and density of the spheroid tissue.

In addition to applications in tissue engineering, this system also has promising characteristics for drug testing applications. Formation time, resulting spheroid size and morphology in 2D and 3D phases might yield useful parameters of early assay readouts with a high sample number, while all standard endpoint assays remain available as additional readouts. The fast and easy generation of large amounts of spheroids also enables applications for high-throughput testing, with lower variation compared to single-well systems, as was shown by the comparison of grid plates to standard pellet cultures. Additionally the easy generation and low variation combined with the controllability of resulting spheroid size make grid plate spheroids interesting 'building blocks' for subsequent biofabrication applications (e.g. bioprinting).

Finally the herein presented system, allows for significant reduction in production and maintenance cost and time. Due to reduced media consumption in comparison to 96-well plates, a reagent expense reduction up to ten-fold is achievable, assuming the generation of 200 spheroids (which is the approximate number of spheroids generated per dish of 6 cm diameter). As the laser engraving method used is very flexible in regard to the cell culture vessel used as 'raw-material', it can be adapted depending on experimental needs, allowing for even better efficiency. This might be of especial interest for labs and industry working with expensive media or additives.

5. Conclusion

In conclusion, a versatile and easy to manufacture culturing system for high-throughput spheroid generation by modification of commercially available standard cell-culture dishes has been presented. Spheroid formation was tested with hAC and ASC/TERT1 and found to be especially efficient with co-cultures of both cell types yielding reproducible diameters while reducing both reagent and time consumption. Furthermore, a comparable but more reproducible differentiation compared to standard pellet culture in a low-dose growth factor chondrogenic differentiation setup was demonstrated. The spheroids generated showed outgrowth with matrix deposition when embedded into hydrogel, thus making it a promising platform for the production of building blocks for tissue regeneration. Due to the high number of produced spheroids and possible early readout parameters during the formation phase, this system might further be a promising tool for high-throughput testing applications.

Acknowledgments

The ASC/TERT1 cell line was kindly provided by Evercyte (Evercyte, Vienna, Austria), Phoenix-Ampho cells were a gift from Regina Grillari (University of Natural Resources and Life Sciences, Vienna, Austria). Furthermore, the authors would like to thank Barbara Schädl for performing histological staining, Claudia Gahleitner for statistical assistance, Severin Mühleder and Wolfgang Holnthoner for support with viral transfections of ASC/TERT1, and Heinz Redl for scientific discussion and critically reading the manuscript.

Funding

The authors would like to acknowledge the funding received from the Austrian Research Promotion Agency (FFG, Grant Number 867720).

Conflict of interest

The authors declare that the research was conducted in the absence of any commercial or financial relationships that could be construed as a potential conflict of interest.

Author contributions

M F: performance of the experiments; M F and S N: writing the manuscript, study design, data analysis; P G: production of grid plates; S W: study design and interpretation of data; all authors critically read and reviewed the manuscript.

ORCID iDs

Marian Fürsatz https://orcid.org/0000-0003-4990-3326
Sylvia Nürnberger https://orcid.org/0000-0002-5175-5118

References

[1] Ruedel A, Hofmeister S and Bosserhoff A-K 2013 Development of a model system to analyze chondrogenic differentiation of mesenchymal stem cells *Int. J. Clin. Exp. Pathol.* **6** 3042–8 (PMID: 24294400)
[2] Panek M, Grabacka M and Pierzchalska M 2018 The formation of intestinal organoids in a hanging drop culture *Cytotechnology* **70** 1–11
[3] Widder M, Lemke K, Kekeç B, Förster T, Grodrian A and Gastrock G 2018 A modified 384-well-device for versatile

use in 3D cancer cell (co-)cultivation and screening for investigations of tumor biology *in vitro Eng. Life Sci.* **18** 132–9
[4] Johnstone B, Hering T M, Caplan A I, Goldberg V M and Yoo J U 1998 In vitrochondrogenesis of bone marrow-derived mesenchymal progenitor cells *Exp. Cell Res.* **238** 265–72
[5] Zhang L, Su P, Xu C, Yang J, Yu W and Huang D 2010 Chondrogenic differentiation of human mesenchymal stem cells: a comparison between micromass and pellet culture systems *Biotechnol. Lett.* **32** 1339–46
[6] Jähn K, Richards R, Archer C and Stoddart M 2010 Pellet culture model for human primary osteoblasts *Eur. Cells Mater.* **20** 149–61
[7] Metzger W, Sossong D, Bächle A, Pütz N, Wennemuth G, Pohlemann T and Oberringer M 2011 The liquid overlay technique is the key to formation of co-culture spheroids consisting of primary osteoblasts, fibroblasts and endothelial cells *Cytotherapy* **13** 1000–12
[8] Greco K V, Iqbal A J, Rattazzi L, Nalesso G, Moradi-Bidhendi N, Moore A R, Goldring M B, Dell'Accio F and Perretti M 2011 High density micromass cultures of a human chondrocyte cell line: a reliable assay system to reveal the modulatory functions of pharmacological agents *Biochem. Pharmacol.* **82** 1919–29
[9] Mello M A and Tuan R S 1999 High density micromass cultures of embryonic limb bud mesenchymal cells: an *in vitro* model of endochondral skeletal development *In Vitro Cell. Dev. Biol. Anim.* **35** 262–9
[10] Tung Y-C, Hsiao A Y, Allen S G, Torisawa Y, Ho M and Takayama S 2011 High-throughput 3D spheroid culture and drug testing using a 384 hanging drop array *Analyst* **136** 473–8
[11] Kowalski M, Raksakulthai V, Prasauckas K and Jones-roe T 2016 Automated 3D cell culture and screening by imaging and flow cytometry *Beckman Coulter (Application Note)* (available at: www.beckman.com/resources/reading-material/application-notes/automated-3d-cell-culture-screening-imaging-flow-cytometry)
[12] Rieger L, Larson B, Ejiri Y, Alms A and Schroeder J 2016 Automation and image-based analysis of a hanging drop micro-hole plate model to create and differentiate 3D mesenchymal stem cell spheroids for downstream tissue formation *BioTek (Application Note)* (https://www.biotek.com/assets/tech_resources/Elplasia%20Tissue%20Generation_App_Note_low%20res1.pdf)
[13] Greve F, Fluri D, Hinterneder J M, Garbow N and Gerwe B 2016 Automation of 3D spheroid production, cell culture and analysis *Perkin Elmer (Application Note)* (https://www.perkinelmer.com/lab-solutions/resources/docs/APP_012829_01Automationof3DSpheroidProductionCellCultureandAnalysis.pdf)
[14] Welter J, Solchaga L and Penick K 2007 Simplification of aggregate culture of human mesenchymal stem cells as a chondrogenic screening assay *Biotechniques* **42** 732–7
[15] Lehmann R, Gallert C, Roddelkopf T, Junginger S and Thurow K 2016 Biomek cell workstation: a flexible system for automated 3D cell cultivation *J. Lab. Autom.* **21** 568–78
[16] Lehmann R, Gallert C, Roddelkopf T, Junginger S, Jonitz-Heincke A, Wree A and Thurow K 2016 Manually and automatically produced pellet cultures of human primary chondrocytes: a comparative analysis *Eng. Life Sci.* **16** 272–82
[17] Larson B, Souza G and Seldin J 2016 An automated walk-away system to perform differentiation of 3D mesenchymal stem cell spheroids *BioTek (Application Note)*
[18] Dean D M, Napolitano A P, Youssef J and Morgan J R 2007 Rods, tori, and honeycombs: the directed self-assembly of microtissues with prescribed microscale geometries *FASEB J.* **21** 4005–12
[19] Napolitano A P, Chai P, Dean D M and Morgan J R 2007 Dynamics of the self-assembly of complex cellular aggregates on micromolded nonadhesive hydrogels *Tissue Eng.* **13** 2087–94
[20] Desroches B R *et al* 2012 Functional scaffold-free 3-D cardiac microtissues: a novel model for the investigation of heart cells *AJP Heart Circ. Physiol.* **302** H2031–42
[21] Babur B K, Ghanavi P, Levett P, Lott W B, Klein T, Cooper-White J J, Crawford R and Doran M R 2013 The interplay between chondrocyte redifferentiation pellet size and oxygen concentration ed X He *PLoS One* **8** e58865
[22] Hardelauf H *et al* 2011 Microarrays for the scalable production of metabolically relevant tumour spheroids: a tool for modulating chemosensitivity traits *Lab Chip* **11** 419–28
[23] Udomluck N, Kim S H, Cho H, Park J Y and Park H 2020 Three-dimensional cartilage tissue regeneration system harnessing goblet-shaped microwells containing biocompatible hydrogel *Biofabrication* **12** 015019
[24] Nürnberger S *et al* 2019 Repopulation of an auricular cartilage scaffold, AuriScaff, perforated with an enzyme combination *Acta Biomater.* **86** 207–22
[25] Mühleder S, Pill K, Schaupper M, Labuda K, Priglinger E, Hofbauer P, Charwat V, Marx U, Redl H and Holnthoner W 2018 The role of fibrinolysis inhibition in engineered vascular networks derived from endothelial cells and adipose-derived stem cells *Stem Cell Res. Ther.* **9** 35
[26] Schindelin J *et al* 2012 Fiji: an open-source platform for biological-image analysis *Nat. Methods* **9** 676–82
[27] Püspöki Z, Storath M, Sage D and Unser M 2016 Transforms and operators for directional bioimage analysis: a survey *Adv. Anat. Embryol. Cell Biol.* **219** 69–93
[28] Rezakhaniha R, Agianniotis A, Schrauwen J T C, Griffa A, Sage D, Bouten C V C, van de Vosse F N, Unser M and Stergiopulos N 2012 Experimental investigation of collagen waviness and orientation in the arterial adventitia using confocal laser scanning microscopy *Biomech. Model. Mechanobiol.* **11** 461–73
[29] Fonck E, Feigl G G, Fasel J, Sage D, Unser M, Rüfenacht D A and Stergiopulos N 2009 Effect of aging on elastin functionality in human cerebral arteries *Stroke* **40** 2552–6
[30] Nelson C M, Jean R P, Tan J L, Liu W F, Sniadecki N J, Spector A A and Chen C S 2005 Emergent patterns of growth controlled by multicellular form and mechanics *Proc. Natl Acad. Sci.* **102** 11594–9
[31] Lee J K, Hu J C Y, Yamada S and Athanasiou K A 2016 Initiation of chondrocyte self-assembly requires an intact cytoskeletal network *Tissue Eng.* A **22** 318–25
[32] Zaleskas J M, Kinner B, Freyman T M, Yannas I V, Gibson L J and Spector M 2004 Contractile forces generated by articular chondrocytes in collagen-glycosaminoglycan matrices *Biomaterials* **25** 1299–308
[33] Schell J Y, Wilks B T, Patel M, Franck C, Chalivendra V, Cao X, Shenoy V B and Morgan J R 2016 Harnessing cellular-derived forces in self-assembled microtissues to control the synthesis and alignment of ECM *Biomaterials* **77** 120–9
[34] Rottmar M, Mhanna R, Guimond-Lischer S, Vogel V, Zenobi-Wong M and Maniura-Weber K 2014 Interference with the contractile machinery of the fibroblastic chondrocyte cytoskeleton induces re-expression of the cartilage phenotype through involvement of PI3K, PKC and MAPKs *Exp. Cell Res.* **320** 175–87
[35] Dong G *et al* 2019 Serum-free culture system for spontaneous human mesenchymal stem cell spheroid formation *Stem Cells Int.* **2019** 6041816
[36] Widelitz R B, Jiang T-X, Murray B A and Chuong C-M 1993 Adhesion molecules in skeletogenesis: II. Neural cell adhesion molecules mediate precartilaginous mesenchymal condensations and enhance chondrogenesis *J. Cell. Physiol.* **156** 399–411
[37] Lee H J, Choi B H, Min B-H and Park S R 2009 Changes in surface markers of human mesenchymal stem cells during the chondrogenic differentiation and dedifferentiation processes *in vitro Arthritis Rheum.* **60** 2325–32

[38] Park I-S, Choi Y J, Kim H-S, Park S-H, Choi B H, Kim J-H, Song B R and Min B-H 2019 Development of three-dimensional articular cartilage construct using silica nano-patterned substrate ed F Gelain *PLoS One* **14** e0208291
[39] Mertz A F, Che Y, Banerjee S, Goldstein J M, Rosowski K A, Revilla S F, Niessen C M, Marchetti M C, Dufresne E R and Horsley V 2013 Cadherin-based intercellular adhesions organize epithelial cell-matrix traction forces *Proc. Natl Acad. Sci.* **110** 842–7
[40] Tsuchiya K, Chen G, Ushida T, Matsuno T and Tateishi T 2004 The effect of coculture of chondrocytes with mesenchymal stem cells on their cartilaginous phenotype *in vitro Mater. Sci. Eng.* C **24** 391–6
[41] Hildner F, Concaro S, Peterbauer A, Wolbank S, Danzer M, Lindahl A, Gatenholm P, Redl H and van Griensven M 2009 Human adipose-derived stem cells contribute to chondrogenesis in coculture with human articular chondrocytes *Tissue Eng.* A **15** 3961–9
[42] Taylor D W, Ahmed N, Hayes A J, Ferguson P, Gross A E, Caterson B and Kandel R A 2012 Hyaline cartilage tissue is formed through the co-culture of passaged human chondrocytes and primary bovine chondrocytes *J. Histochem. Cytochem.* **60** 576–87
[43] Gan L and Kandel R A 2007 *In vitro* cartilage tissue formation by co-culture of primary and passaged chondrocytes *Tissue Eng.* **13** 831–42
[44] Pleumeekers M M, Nimeskern L, Koevoet J L M, Karperien M, Stok K S and van Osch G J V M 2018 Trophic effects of adipose-tissue-derived and bone-marrow-derived mesenchymal stem cells enhance cartilage generation by chondrocytes in co-culture *PLoS One* **13** 1–23
[45] Meretoja V, Dahlin L, Kasper F K and Mikos A G 2012 Enhanced chondrogenesis in co-cultures with articular chondrocytes and mesenchymal stem cells *Biomaterials* **33** 6362–9
[46] Bian W and Nenad B 2009 Tissue engineering of functional skeletal muscle: challenges and recent advances *IEEE Eng. Med. Biol. Mag.* **27** 109–13
[47] Grassel S, Rickert M, Opolka A, Bosserhoff A, Angele P, Grifka J and Anders S 2010 Coculture between periosteal explants and articular chondrocytes induces expression of TGF-1 and collagen I *Rheumatology* **49** 218–30
[48] Gardner O, Fahy N, Alini M and Stoddart M 2016 Differences in human mesenchymal stem cell secretomes during chondrogenic induction *Eur. Cells Mater.* **31** 221–35
[49] Li Z, Kupcsik L, Yao S-J, Alini M and Stoddart M J 2010 Mechanical load modulates chondrogenesis of human mesenchymal stem cells through the TGF-β pathway *J. Cell. Mol. Med.* **14** 1338–46
[50] Takigawa M, Okawa T, Pan H-O, Aoki C, Takahashi K, Zue J-D, Suzuki F and Kinoshita A 1997 Insulin-like growth factors I and II are autocrine factors in stimulating proteoglycan synthesis, a marker of differentiated chondrocytes, acting through their respective receptors on a clonal human chondrosarcoma-derived chondrocyte cell line, HCS-2/8 1 *Endocrinology* **138** 4390–400
[51] Haque A, Gheibi P, Gao Y, Foster E, Son K J, You J, Stybayeva G, Patel D and Revzin A 2016 Cell biology is different in small volumes: endogenous signals shape phenotype of primary hepatocytes cultured in microfluidic channels *Sci. Rep.* **6** 33980
[52] Guild J, Haque A, Gheibi P, Gao Y, Son K J, Foster E, Dumont S and Revzin A 2016 Embryonic stem cells cultured in microfluidic chambers take control of their fate by producing endogenous signals including LIF *Stem Cells* **34** 1501–12
[53] Kushida A, Yamato M, Konno C, Kikuchi A, Sakurai Y and Okano T 1999 Decrease in culture temperature releases monolayer endothelial cell sheets together with deposited fibronectin matrix from temperature-responsive culture surfaces *J. Biomed. Mater. Res.* **45** 355–62
[54] Kobayashi J, Kikuchi A, Aoyagi T and Okano T 2019 Cell sheet tissue engineering: cell sheet preparation, harvesting/manipulation, and transplantation *J. Biomed. Mater. Res.* A **107** 955–67
[55] Moreira Teixeira L, Leijten J, Sobral J, Jin R, van Apeldoorn A, Feijen J, van Blitterswijk C, Dijkstra P and Karperien M 2012 High throughput generated micro-aggregates of chondrocytes stimulate cartilage formation *in vitro* and *in vivo Eur. Cells Mater.* **23** 387–99
[56] de Moor L, Fernandez S, Vercruysse C, Tytgat L, Asadian M, de Geyter N, van Vlierberghe S, Dubruel P and Declercq H 2020 Hybrid bioprinting of chondrogenically induced human mesenchymal stem cell spheroids *Front. Bioeng. Biotechnol.* **8** 1–20
[57] Lee J-I, Sato M, Kim H-W and Mochida J 2011 Transplantation of scaffold-free spheroids composed of synovium-derived cells and chondrocytes for the treatment of cartilage defects of the knee *Eur. Cells Mater.* **22** 275–90
[58] Huang G-S, Tseng C-S, Linju Yen B, Dai L-G, Hsieh P-S and Hsu S 2013 Solid freeform-fabricated scaffolds designed to carry multicellular mesenchymal stem cell spheroids for cartilage regeneration *Eur. Cells Mater.* **26** 179–94
[59] Eschen C, Kaps C, Widuchowski W, Fickert S, Zinser W, Niemeyer P and Roël G 2020 Clinical outcome is significantly better with spheroid-based autologous chondrocyte implantation manufactured with more stringent cell culture criteria *Osteoarthr. Cartilage Open* **2** 100033